

Bit-Metric Decoding Rate in Multi-User MIMO Systems: Applications

K. Pavan Srinath and Jakob Hoydis, *Senior Member, IEEE*

Abstract

This is the second part of a two-part paper that focuses on link-adaptation (LA) and physical layer (PHY) abstraction for multi-user MIMO (MU-MIMO) systems with non-linear receivers. The first part proposes a new metric, called bit-metric decoding rate (BMDR) for a detector, as being the equivalent of post-equalization signal-to-interference-noise ratio (SINR) for non-linear receivers. Since this BMDR does not have a closed form expression, a machine-learning based approach to estimate it effectively is presented. In this part, the concepts developed in the first part are utilized to develop novel algorithms for LA, dynamic detector selection from a list of available detectors, and PHY abstraction in MU-MIMO systems with arbitrary receivers. Extensive simulation results that substantiate the efficacy of the proposed algorithms are presented.

Index Terms

Bit-metric decoding rate (BMDR), convolutional neural network (CNN), linear minimum mean square error (LMMSE), link-adaptation (LA), K -best detector, multi-user MIMO (MU-MIMO), orthogonal frequency division multiplexing (OFDM), physical layer (PHY) abstraction.

I. INTRODUCTION

In the first part [1] of this two-part paper, we introduced the notion of bit-metric decoding rate (BMDR) for each user in a multi-user MIMO (MU-MIMO) system with any arbitrary detector. BMDR is an information-theoretic measure that takes into consideration the effect of a possibly suboptimal detector. Since BMDR doesn't have a closed form expression that would allow its instantaneous calculation, we described a machine-learning based solution to predict it for an

K. P. Srinath is with Nokia Bell Labs, 91620 Nozay, France (email: pavan.koteshwar_srinath@nokia-bell-labs.com), and J. Hoydis is with NVIDIA, 06906 Sophia Antipolis, France (email: jhoydis@nvidia.com). A significant part of this work was done when J. Hoydis was at Nokia Bell Labs, 91620 Nozay, France.

observed set of channel realizations. In the second part of this two-part paper, we use the concepts developed in the first part to address two important problems in MU-MIMO systems that are detailed below:

A. Uplink link-adaptation

In 5G New Radio (5G NR), when a user-equipment (UE) wishes to send data to the base station (BS), it makes a scheduling request on the physical random access channel (PRACH) for the first time, or on the physical uplink control channel (PUCCH) if already scheduled. The BS then sends an uplink grant in the downlink control information (DCI) message with information on what physical resource blocks (PRBs) to use, and what modulation and coding scheme (MCS) to use for data transmission. The method to determine what MCS to use is at the discretion of the BS. Following this uplink grant, the UE sends data using the mentioned MCS on the physical uplink shared channel (PUSCH). This process is part of link-adaptation (LA), where the BS adapts the MCS levels according to the capacity of the link between the UE and itself.

Some of the best known works on LA are [2]–[4], and one can refer to references therein for a comprehensive survey of the state-of-the-art on the topic. All known works in the literature propose to perform outer loop link adaptation (OLLA). OLLA is a technique where the signal-to-interference-noise ratio (SINR) is initially estimated, and then a correction to this SINR estimate is performed to account for any estimation inaccuracy. This correction is dependent on the number of correctly/incorrectly decoded codewords (through ACK/NACK on the downlink for downlink LA). Next, the most appropriate MCS level is chosen based on this corrected SINR.

In a MU-MIMO system, the principles of OLLA can still be used, and work well when the users are involved in large file transfers. This is especially true for linear receivers (like the linear minimum mean square error (LMMSE) detector [5, Ch. 8]) that allow the computation of a post-equalization SINR. However, the known MCS selection techniques that are based on post-equalization SINR do not work in systems with non-linear detectors like sphere-decoder [6], [7] and its fixed-complexity variants [8], [9]. For such systems, LA is an open problem.

B. Physical layer abstraction

Telecommunication chip manufacturers use system-level simulations (SLS) to evaluate the performance of their algorithms. A typical simulator consists of (but is not limited to) the

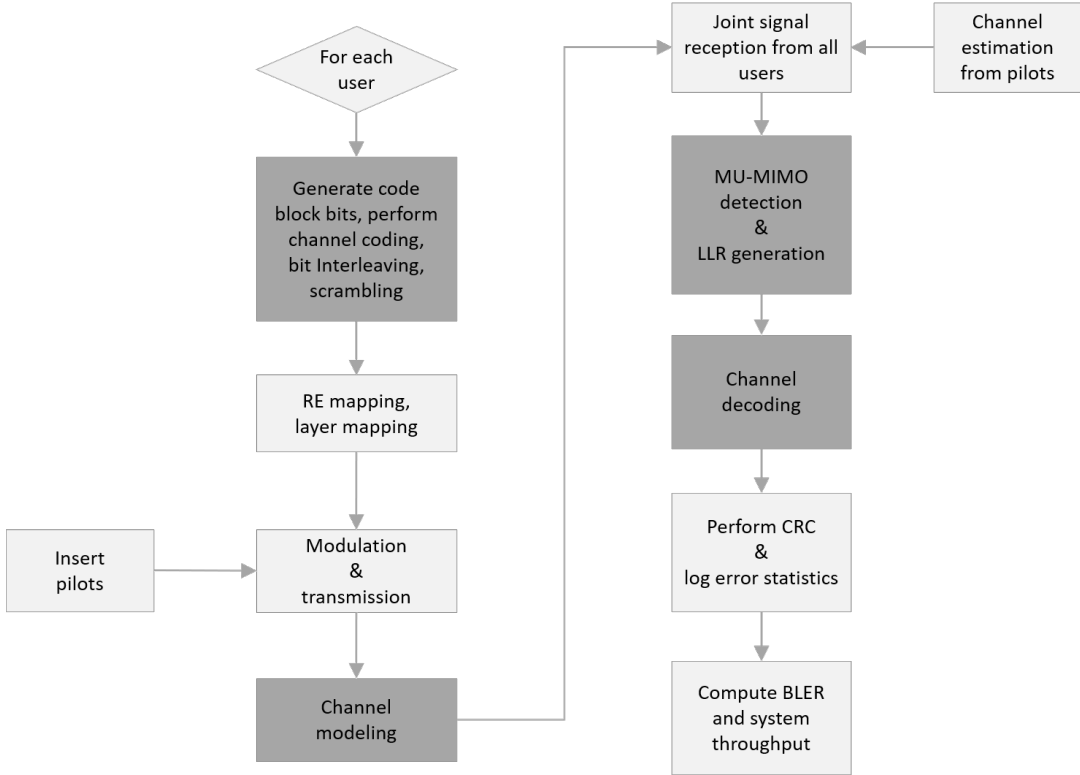


Fig. 1: Flowchart of a full MU-MIMO link level simulation. The darkly shaded boxes represent the time-intensive procedures.

following functionalities: intercell-interference modeling, resource scheduling and allocation, power allocation and power control, LA block with channel quality feedback, channel modeling, link performance modeling. Of these, the link performance-modeling block is the one that models the physical layer components of the communication system. The flowchart of a typical link-level simulation is depicted in Fig. 1. The boxes that are darkly shaded refer to the operations that are time-intensive/resource-intensive to execute, and these include (but are not limited to) code-block (CB) segmentation, channel-coding, bit-interleaving, and scrambling at the transmitter side, and multiple-input multiple-output (MIMO) detection with log-likelihood ratio (LLR) generation, and channel decoding at the receiver side. Therefore, in order to reduce the complexity of SLS, these components are replaced by simpler functionalities that are quicker to execute but capture the essential behavior of the overall physical layer. This technique is called physical layer (PHY) abstraction. To be precise, the goal of link performance modeling (or equivalently, PHY abstraction) is to obtain the same figures of merit for performance evaluation as would be

obtained if the original components were used, but with much simpler complexity. The commonly used figures of merit are system throughput and codeword error rate (CER) or block error rate (BLER), noting that a block can consist of multiple codewords [10, Section 5].

In the literature, there exist several abstraction models for the case of single-user SISO (SU-SISO) systems, and (with some limitations) for MIMO systems with linear receivers. A few papers on this topic are [11]–[13] and references therein. The limitations of the approaches in these papers are the following:

- For linear detectors, these papers propose to compress the set of post-equalization SINRs obtained at the receiver over every resource element (RE) into an effective SINR, and then map this effective SINR to a BLER using an approximate SINR-BLER lookup table. This compression of several post-equalization SINRs to a single effective SINR is known as effective SINR metric (ESM). There are several such metrics in the literature: exponential ESM (EESM), mutual-information ESM (MIESM), capacity ESM (CESM), and logarithmic ESM (LESM). A variant of MIESM, known as received bit information rate (RBIR), is proposed for usage in IEEE 802.11 while 3GPP recommends EESM. However, there is no clear consensus on the selection of a single method.
- For MIMO systems with non-linear detectors, there is no known technique in the literature to perform PHY abstraction.

These limitations are addressed in this part of the two-part paper. The summary of our contributions is listed below:

- We describe a new algorithm (Section IV) for performing LA in MU-MIMO systems for arbitrary detectors. This algorithm makes use of BMDR in lieu of post-equalization SINR.
- We present a technique to dynamically select the most appropriate detector from a list of available detectors (Section IV-A).
- We propose a new method (Section V) for performing PHY abstraction in MU-MIMO systems with arbitrary receivers.
- Extensive simulation results are provided to verify the efficacy of the proposed techniques.

Paper Organization

The system model and a few relevant definitions are presented in Section II. Section III explains the technique to obtain a BMDR-CER map. Section IV presents a new algorithm for LA and dynamic detector selection while Section V describes a new technique to perform PHY

abstraction. Simulation results showing the efficacy of proposed techniques are presented in Section VI, and the concluding remarks are made in Section VII.

Notation

Boldface upper-case (lower-case) letters denote random matrices (vectors), and normal upright upper-case (lower-case) letters are understood from context to denote the realizations of random matrices (vectors). The field of complex numbers and the field of real numbers are respectively denoted by \mathbb{C} and \mathbb{R} . The notation $\mathbf{X} \in \mathcal{S}^{m \times n}$ denotes that \mathbf{X} is a matrix of size $m \times n$ with each entry taking values from a set \mathcal{S} . The identity matrix of size $n \times n$ is denoted by \mathbf{I}_n . The notation $\mathbf{n} \sim \mathcal{CN}(0, \mathbf{I}_n)$ denotes that \mathbf{n} is sampled from the n -dimensional complex standard normal distribution.

II. SYSTEM MODEL AND DEFINITIONS

We consider an orthogonal frequency division multiplexing (OFDM) based MU-MIMO uplink transmission as in the first part [1, Section II], and reiterate the signal model below.

$$\mathbf{y}_{f,t} = \sum_{i=1}^{N_u} \sqrt{\frac{\rho_i}{n_t^{(i)}}} \mathbf{H}_{f,t,i} \mathbf{s}_{f,t,i} + \mathbf{n}_{f,t} = \mathbf{H}_{f,t} \mathbf{s}_{f,t} + \mathbf{n}_{f,t} \quad (1)$$

where $\mathbf{y}_{f,t} \in \mathbb{C}^{n_r \times 1}$ is the received signal vector at the BS equipped with n_r receive antennas, $\mathbf{H}_{f,t,i} \in \mathbb{C}^{n_r \times N}$ is the MIMO channel from UE i to the BS with UE i having $n_t^{(i)}$ transmit antennas and total transmit power ρ_i , $\mathbf{s}_{f,t,i} \in \mathcal{Q}_i^{n_t^{(i)} \times 1}$ is the transmitted signal vector from UE i with each entry taking values from a constellation \mathcal{Q}_i , $\mathbf{H}_{f,t} \triangleq \left[\sqrt{\rho_1/n_t^{(1)}} \mathbf{H}_{f,t,1}, \dots, \sqrt{\rho_{N_u}/n_t^{(N_u)}} \mathbf{H}_{f,t,N_u} \right] \in \mathbb{C}^{n_r \times N}$ is the composite MU-MIMO channel with $N = \sum_{i=1}^{N_u} n_t^{(i)}$, $\mathbf{s}_{f,t} \triangleq [\mathbf{s}_{f,t,1}^T, \dots, \mathbf{s}_{f,t,N_u}^T]^T \in \mathcal{Q}^{N \times 1}$ the composite transmitted signal vector with $\mathcal{Q}^{N \times 1} \triangleq \mathcal{Q}_1^{n_t^{(1)} \times 1} \times \dots \times \mathcal{Q}_{N_u}^{n_t^{(N_u)} \times 1}$, and $\mathbf{n}_{f,t} \sim \mathcal{CN}(0, \mathbf{I}_{n_r})$ represents the complex additive white Gaussian noise (AWGN). The subscript (f, t) denotes the (subcarrier, time) indices of the RE in which $\mathbf{y}_{f,t}$ is received.

In practice, there will be intercell-interference (from neighboring cell users) and imperfect channel estimation at the serving BS. Let $\hat{\mathbf{H}}_{f,t}$ denote the estimated channel so that $\mathbf{H}_{f,t} = \hat{\mathbf{H}}_{f,t} + \Delta \mathbf{H}_{f,t}$ where $\Delta \mathbf{H}_{f,t}$ denotes the estimation error. The signal model of (1) in the presence of interference noise from neighboring cells can be written as

$$\mathbf{y}_{f,t} = \hat{\mathbf{H}}_{f,t} \mathbf{s}_{f,t} + \Delta \mathbf{H}_{f,t} \mathbf{s}_{f,t} + \mathbf{n}_{f,t} \quad (2)$$

where the interference noise is subsumed in $\mathbf{n}_{f,t}$ so that $\mathbf{n}_{f,t} \sim \mathcal{CN}(0, \mathbf{K}_n)$ with $\mathbf{K}_n \in \mathbb{C}^{n_r \times n_r}$ being a (known) Hermitian, positive-definite but non-diagonal matrix. Assuming that an LMMSE estimator is used for channel estimation with a known estimation-error covariance of \mathbf{K}_e , we arrive at the following signal model (refer [1, Section III-A] for details) after noise-whitening.

$$\mathbf{y}'_{f,t} = \mathbf{H}'_{f,t} \mathbf{s}_{f,t} + \mathbf{n}'_{f,t} \quad (3)$$

where $\mathbf{y}'_{f,t} = (\mathbf{K}_n + \mathbf{K}_e)^{-\frac{1}{2}} \mathbf{y}_{f,t}$, $\mathbf{H}'_{f,t} = (\mathbf{K}_n + \mathbf{K}_e)^{-\frac{1}{2}} \hat{\mathbf{H}}_{f,t}$, and $\mathbf{n}'_{f,t} \sim \mathcal{CN}(0, \mathbf{I}_{n_r})$ due to the noise-whitening. Therefore, unless specified otherwise, the assumed signal model is that of (1), and any other realistic model can be converted to this form.

Let the constellation \mathcal{Q}_i of UE i be of size 2^{m_i} , and let $b_{f,t,i,l,j}$ denote the j^{th} transmitted bit of UE i on its l^{th} transmit antenna (a detailed system model is available in [1, Section II]). Suppose that a MU-MIMO detector \mathcal{D} is used to generate the LLR for each $b_{f,t,i,l,j}$, $i = 1, \dots, N_u$, $j = 1, \dots, m_i$, $l = 1, \dots, n_t^{(i)}$. Let $q_{\mathcal{D}}(b_{f,t,i,l,j}; \mathbf{y}_{f,t}, \mathbf{H}_{f,t})$ denote the posterior probability $\mathbb{P}\{b_{f,t,i,l,j} | \mathbf{y}_{f,t}, \mathbf{H}_{f,t}, \mathcal{D}\}$ obtained from the generated LLR for $b_{f,t,i,l,j}$.

Definition II.1. *BMDR [1, Section III]: The BMDR of \mathcal{D} for UE i , which is denoted by $R_{\mathcal{D},i}(\mathcal{H})$, for a set of channels \mathcal{H} (this set can be a singleton with just a single channel matrix) is defined as follows:*

$$\begin{aligned} R_{\mathcal{D},i}(\mathcal{H}) &\triangleq 1 + \frac{1}{|\mathcal{H}|} \sum_{\mathbf{H}_{f,t} \in \mathcal{H}} \mathbb{E}_{\mathbf{y}_{f,t} | \mathbf{H}_{f,t}} \left[\frac{1}{m_i n_t^{(i)}} \sum_{l=1}^{n_t^{(i)}} \sum_{j=1}^{m_i} \log_2 (q_{\mathcal{D}}(b_{f,t,i,l,j}; \mathbf{y}_{f,t}, \mathbf{H}_{f,t})) \middle| \mathbf{H}_{f,t} \right] \quad (4) \\ &= \frac{1}{|\mathcal{H}|} \sum_{\mathbf{H}_{f,t} \in \mathcal{H}} R_{\mathcal{D},i}(\mathbf{H}_{f,t}) \end{aligned}$$

where $\{b_{f,t,i,l,j}\}_{j=1}^{m_i}$ is related to the l^{th} element of $\mathbf{s}_{f,t,i}$ through the bijective map that assigns groups of m_i bits to a constellation signal in \mathcal{Q}_i for each $l = 1, \dots, n_t^{(i)}$, and $\mathbf{y}_{f,t}$ is dependent only on $\mathbf{s}_{f,t}$ and $\mathbf{n}_{f,t}$ when conditioned on $\mathbf{H}_{f,t}$. Note that $R_{\mathcal{D},i}(\mathcal{H})$ is itself a random variable whose realization is dependent on the realizations of the channel matrices $\mathbf{H}_{f,t}$.

Suppose that UE i uses a length- n_i , rate- r_i channel code whose codeword bits are transmitted over a set of REs \mathcal{G}_i with the corresponding set of channel realizations $\mathcal{H}_{\mathcal{G}_i} = \{\mathbf{H}_{f,t}, (f, t) \in \mathcal{G}_i\}$. In the rest of the paper, we focus only on quadrature amplitude modulation (QAM) due to its significance in most wireless communications standards; so, the modulation order m specifies 2^m -QAM. Let $\mathbf{m} \triangleq \{m_1, \dots, m_{N_u}\}$ be the set of modulation orders used by all the co-scheduled users. To emphasize that the BMDR depends on \mathbf{m} , we use a slight change of notation from (4),

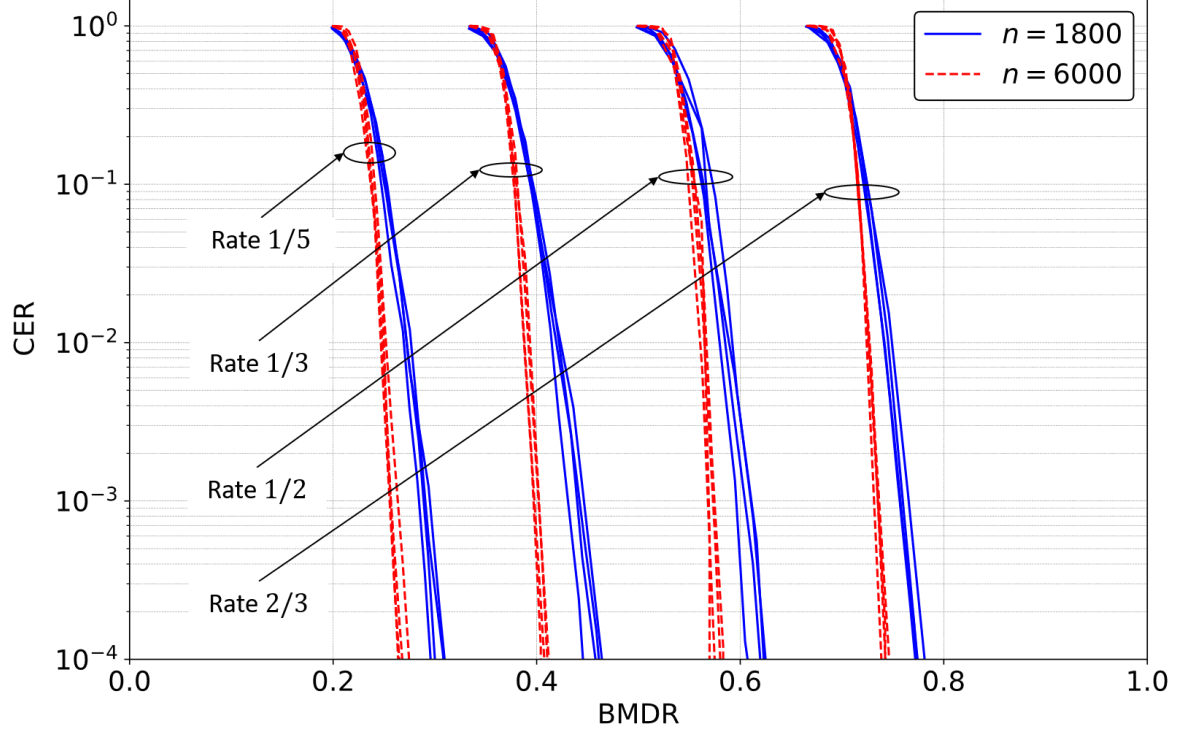


Fig. 2: BMDR vs CER for the single-input single-output (SISO)-AWGN channel using 4/16/64/256-QAM and different code-rates. The solid blue lines correspond to a length-1800 5G-LDPC code while the dashed red lines correspond to a length-6000 5G-LDPC code.

and denote the BMDR of UE i for an observed channel realization $H_{f,t}$ by $R_{\mathcal{D},i}(\mathbf{m}, H_{f,t})$, and that for $\mathcal{H}_{\mathcal{G}_i}$ by $R_{\mathcal{D},i}(\mathbf{m}, \mathcal{H}_{\mathcal{G}_i}) = \frac{1}{|\mathcal{G}_i|} \sum_{(f,t) \in \mathcal{G}_i} R_{\mathcal{D},i}(\mathbf{m}, H_{f,t})$. The result of [1, Theorem 1] is that in order to achieve a low CER, it is necessary that $R_{\mathcal{D},i}(\mathbf{m}, \mathcal{H}_{\mathcal{G}_i}) > r_i$. Even though $R_{\mathcal{D},i}(\mathbf{m}, \mathcal{H}_{\mathcal{G}_i})$ cannot be known in advance, its value can be predicted from the most recent observations of the channel. This is the main idea behind the usage of BMDR for LA.

III. MAPPING BMDR TO CER

Before detailing the algorithm for LA, it is necessary to describe a method to map BMDR to CER. The proof of [1, Theorem 1] suggests that CER has a strong inverse relationship with the codeword length n_i and the margin $\delta_i = R_{\mathcal{D},i}(\mathbf{m}, \mathcal{H}_{\mathcal{G}_i}) - r_i$, and a weak direct relationship with $m_i = \log_2(|\mathcal{Q}_i|)$. Figure 2 shows the plots of the CER as a function of BMDR for the SISO-AWGN channel with maximum-likelihood detector (MLD), for length-1800 and length-6000 5G-low-density parity-check (LDPC) codes of various rates. The plots have been numerically

obtained for 4/16/64/256–QAM (with the smaller constellation slightly better than the larger constellation). *It is to be noted that this BMDR multiplied by m is well-known in the literature as the capacity of bit-interleaved coded modulation (BICM) for 2^m –QAM [14].* The plots agree with the inference about the strong dependence of CER on n_i and δ , and the weak dependence on m_i .

We propose to generate a lookup table using simulations performed on a SISO AWGN channel. We expect this lookup table to be relevant even to the case of MU-MIMO because the proof of [1, Theorem 1] suggests that the error behavior of a coding scheme depends predominantly on BMDR alone. In the rest of the paper, to distinguish between codes from the same family (like the 5G-LDPC codes), we explicitly state the rate and length; so $\mathcal{C}(r, n)$ denotes a code with rate r and length n . Let $\mathcal{R}(m, \mathcal{C}(r, n), \epsilon)$ denote the target BMDR required to be guaranteed of a CER of at most ϵ for the SISO-AWGN channel using 2^m –QAM, $\mathcal{C}(r, n)$, and MLD. With this, for a low target probability of codeword error ϵ ($< 10^{-1}$), we can expect the following.

- 1) $\mathcal{R}(m, \mathcal{C}(r, n_1), \epsilon) \leq \mathcal{R}(m, \mathcal{C}(r, n_2), \epsilon)$ if $n_1 > n_2$.
- 2) $\mathcal{R}(m_1, \mathcal{C}(r, n), \epsilon) \approx \mathcal{R}(m_2, \mathcal{C}(r, n), \epsilon)$ if $m_1 > m_2$.

Algorithm 1 provides pseudocode for the lookup table generation technique. In the algorithm, BMDR is empirically calculated using the method outlined in [1, Algorithm 1], but for a SISO-AWGN channel. Since the effect of QAM size on the target BMDR appears to be very small, one can use just QPSK in Algorithm 1 instead of higher dimensional 2^m –QAM in order to reduce the computational complexity. Having generated the lookup table \mathcal{L}_U as detailed in Algorithm 1, $\mathcal{R}(m, \mathcal{C}(r, n), \epsilon)$ for a target CER of ϵ can be obtained from \mathcal{L}_U as

$$\mathcal{R}(m, \mathcal{C}(r, n), \epsilon) = \min_{(R_{MLD}, P_e) \in \mathcal{L}_U} \{R_{MLD} \mid P_e \leq \epsilon\}. \quad (5)$$

It is common to have several choices for the code-length n for a given code-rate r . For example, in 5G NR, $k \in \{1, 8448\}$ [10, Section 5] so that $1/r \leq n \leq 8448/r$. It would be practically infeasible to generate a lookup table for each combination of n and r . Instead, one can compute $\mathcal{R}(m, \mathcal{C}(r, n), \epsilon)$ for $n = n_{min}, n_{max}$, and for a few values of n between n_{max} and n_{min} , where n_{max} and n_{min} denote the maximum and minimum code-lengths, respectively. From these computed values, any target BMDR for intermediate lengths ($n_{min} < n < n_{max}$) can be estimated by linear or polynomial interpolation. We do not go into the details of this, and assume that for any target CER ϵ , code-rate r , modulation order m , and code-length $n_{min} \leq n \leq n_{max}$,

Algorithm 1 Pseudocode to generate a look-up table that maps AWGN BMDR to CER

Input

$\mathcal{C}(r, n)$: Channel code with code-rate r and length n
 m : Modulation order used, implies 2^m -QAM
 \mathfrak{P} : Discrete set of usable signal-to-noise ratio (SNR) values in dB,

$$\mathfrak{P} = \left\{ \rho_{min} + l\Delta\rho, \quad l = 0, 1, \dots, \left\lfloor \frac{\rho_{max} - \rho_{min}}{\Delta\rho} \right\rfloor \right\}$$

Output

\mathcal{L}_U : Look-up table containing BMDR-CER pairs

Initialize

$\mathcal{L}_U \leftarrow \{\}$

for all $\rho \in \mathfrak{P}$ **do**

/* Empirically compute CER for SISO-AWGN channel with channel code $\mathcal{C}(r, n)$,

2^m -QAM, and maximum-likelihood detection at an SNR of ρ dB */

$P_e \leftarrow \text{CER}(\text{SISO-AWGN}, 2^m\text{-QAM}, \mathcal{C}(r, n), \rho)$

/* Empirically compute BMDR for SISO-AWGN channel with 2^m -QAM and

maximum-likelihood detection at an SNR of ρ dB */

$R_{MLD} \leftarrow \text{BMDR}(\text{SISO-AWGN}, 2^m\text{-QAM}, \rho)$

$\mathcal{L}_U \leftarrow \mathcal{L}_U \cup \{(R_{MLD}, P_e)\}$

end for

there exists a (possibly learned) function \mathcal{R} which outputs the estimated target BMDR for $\mathcal{C}(r, n)$ when a 2^m -QAM is used.

IV. LINK-ADAPTATION IN MU-MIMO SYSTEMS

Let \mathcal{M} denote the set of available modulation orders, and $\mathcal{R}(m)$ denote the set of available code-rates for m . We also assume for the sake of simplicity that the codewords of all the users are to be transmitted over the same set of REs with the corresponding set of channel realizations denoted by \mathcal{H}_{next} . This means that if UE i selects a modulation order m_i , the code-length of the channel code that it uses is $|\mathcal{H}_{next}|m_i n_t^{(i)}$. Assuming the usage of an arbitrary detector \mathcal{D} and a target CER of $\underline{\epsilon}$ for all users, MCS selection aims to solve the following joint spectral efficiency

(SE)-maximizing problem.

$$\{(m_i^*, r_i^*)\}_{i=1}^{N_u} = \arg \max_{\{m_i \in \mathcal{M}, r_i \in \mathcal{R}(m_i)\}_{i=1}^{N_u}} \left\{ \frac{1}{N_u} \sum_{i=1}^{N_u} r_i m_i \mid R_{\mathcal{D},i}(\mathbf{m}, \mathcal{H}_{next}) \geq \mathcal{R}(m_i, \mathcal{C}(r_i, n_i), \underline{\epsilon}) \right\} \quad (6)$$

where, as before, $\mathbf{m} = \{m_1, \dots, m_{N_u}\}$. However, we do not yet have the estimates of the channel matrices of \mathcal{H}_{next} , and can only rely on the most recent past-channel estimates. In 5G NR, these can be the channel estimates obtained using demodulation reference signals (DMRSs) in the previous transmission slot for those users that have already transmitted, or using sounding reference signals (SRSs) if there was no transmission in the previous slot. We denote the set of these channel estimates by $\widehat{\mathcal{H}}$. Using a trained BMDR-predictor (detailed in [1, Section V] for both linear and non-linear detectors), the BMDR for UE i can be predicted for $\widehat{\mathcal{H}}$ as $\hat{R}_{\mathcal{D},i}(\mathbf{m}, \widehat{\mathcal{H}})$. However, since these are estimates on a possibly outdated set of channel estimates, we need a BMDR-correction offset δ_i for each UE i . This correction offset is similar to the SINR-correction offset in OLLA, and it captures the amount of confidence one has in the estimated BMDR; the greater the confidence, the closer δ_i is to 0. In case the BMDR is underestimated, a positive δ_i acts as a correction. In large file transfers, δ_i typically varies throughout the transmission; decreasing by a large value for every incorrectly decoded codeword, and increasing by a small value otherwise. With this, the practical MCS-selection problem can be restated as

$$\{(m_i^*, r_i^*)\}_{i=1}^{N_u} = \arg \max_{\{m_i \in \mathcal{M}, r_i \in \mathcal{R}(m_i)\}_{i=1}^{N_u}} \left\{ \frac{1}{N_u} \sum_{i=1}^{N_u} r_i m_i \mid \hat{R}_{\mathcal{D},i}(\mathbf{m}, \widehat{\mathcal{H}}) \geq \mathcal{R}(m_i, \mathcal{C}(r_i, n_i), \underline{\epsilon}) - \delta_i \right\}. \quad (7)$$

Algorithm 2 provides pseudocode to efficiently solve (7). Note that when calculating r_i^* for a chosen m_i^* , if there is no $r_i \in \mathcal{R}(m_i^*)$ satisfying $\hat{R}_{\mathcal{D},i}(\mathbf{m}, \widehat{\mathcal{H}}) \geq \mathcal{R}(m_i^*, \mathcal{C}(r_i, n_i), \underline{\epsilon}) - \delta_i$, we choose $r_i^* = \min \mathcal{R}(m_i^*)$.

A. Dynamic Detector Selection

Suppose that there are N_d available detectors $\{\mathcal{D}_p\}_{p=1}^{N_d}$ to choose from, with the complexity of \mathcal{D}_p denoted by $\mathfrak{C}(\mathcal{D}_p)$. We emphasize here that the complexity could either be in terms of time taken to perform detection for one RE, or in terms of the number of computations performed during the course of detection for one RE. The two need not be proportional to one another, an example being the case where a particular detector performs more operations than its rival but allows parallel processing while its rival does not. Depending on the application, the complexity

Algorithm 2 Pseudocode to select MCS for each user based on channel measurements

Input

\mathcal{M} : Set of available QAM modulation orders, $\mathcal{M} = \{2k, k = 1, \dots, k_{max}\}$
 $\mathcal{R}(m)$: Set of available code-rates for modulation order m , $\forall m \in \mathcal{M}$
 \mathcal{R} : Learned function to predict the target BMDR for a target CER $\underline{\epsilon}$ given
 code-rate r , code-length n , modulation order m
 δ_i : Precomputed BMDR-correction offset for UE i , $\forall i = 1, \dots, N_u$
 $\hat{\mathcal{H}}$: Set of estimated composite MU-MIMO channel matrices of size $n_r \times N$
 n_{RE} : Number of REs for codeword transmission
 $f_{\mathcal{D},i}$: A pretrained BMDR-predictor for detector \mathcal{D} and UE i , $\forall i = 1, \dots, N_u$,
 takes as inputs the channel matrix and set of modulation orders for all users

Output

mcs_i : Chosen MCS index for UE i , $\forall i = 1, \dots, N_u$

Initialize

$\text{updateFlag} \leftarrow \text{True}$
 $c_i \leftarrow k_{max}, \forall i = 1, \dots, N_u$ \triangleright Begin with the highest modulation order

while updateFlag is True **do**

$m_i \leftarrow 2c_i, n_i \leftarrow n_{RE}m_i n_t^{(i)}, \forall i = 1, \dots, N_u$ \triangleright Assign modulation order to user

$\mathfrak{m} \leftarrow \{m_1, \dots, m_{N_u}\}$

$\hat{R}_{\mathcal{D},i}(\mathfrak{m}, \hat{\mathcal{H}}) \leftarrow \frac{1}{|\hat{\mathcal{H}}|} \sum_{\hat{\mathcal{H}} \in \hat{\mathcal{H}}} f_{\mathcal{D},i}(\mathfrak{m}, \hat{\mathcal{H}}), \forall i = 1, \dots, N_u$ \triangleright Estimate average BMDR

for all $i = 1, \dots, N_u$ **do**

if $\hat{R}_{\mathcal{D},i}(\mathfrak{m}, \hat{\mathcal{H}}) < \min_{r_i \in \mathcal{R}(m_i)} \{\mathcal{R}(m_i, \mathcal{C}(r_i, n_i), \underline{\epsilon})\} - \delta_i$ **then**

$c_{i,next} \leftarrow \max(c_i - 1, 1)$ \triangleright Reduce modulation order

end if

end for

if $c_{i,next} = c_i, \forall i = 1, \dots, N_u$ **then**

$\text{updateFlag} \leftarrow \text{False}$ \triangleright No more updates of modulation orders

end if

$c_i \leftarrow c_{i,next}, \forall i = 1, \dots, N_u$

end while

$m_i^* \leftarrow m_i, r_i^* \leftarrow \arg \max_{r_i \in \mathcal{R}(m_i)} \{\hat{R}_{\mathcal{D},i}(\mathfrak{m}, \hat{\mathcal{H}}) \geq \mathcal{R}(m_i, \mathcal{C}(r_i, n_i), \underline{\epsilon}) - \delta_i\}, \forall i = 1, \dots, N_u$

$mcs_i \leftarrow \text{MCS}(m_i^*, r_i^*), \forall i = 1, \dots, N_u$ \triangleright Map (m_i^*, r_i^*) to MCS index

metric is chosen such that a less "complex" detector is more desirable for usage than its rival if both the detectors are equally reliable. The list of detectors $\{\mathcal{D}_1, \dots, \mathcal{D}_{N_d}\}$ is assumed to be ordered so that $\mathfrak{C}(\mathcal{D}_1) \leq \dots \leq \mathfrak{C}(\mathcal{D}_{N_d})$. Let $m_{\mathcal{D}_p,i}^*$ and $r_{\mathcal{D}_p,i}^*$ respectively denote the estimated modulation order and code-rate for UE i with detector \mathcal{D}_p according to Algorithm 2. Then, one can use a hybrid detection strategy that dynamically chooses \mathcal{D}_{p^*} where

$$p^* = \min \left\{ \arg \max_{p \in \{1, \dots, N_d\}} \left\{ \frac{1}{N_u} \sum_{i=1}^{N_u} r_{\mathcal{D}_p,i}^* m_{\mathcal{D}_p,i}^* \right\} \right\}. \quad (8)$$

This problem under a different formulation has been considered before in [15]–[17], but our proposed technique is a more natural way of selecting a detector.

V. PHYSICAL LAYER ABSTRACTION

With the system model as described in Section II, assume that UE i transmits the codeword bits on n_{RE} REs, each RE indexed by the frequency-time pair (f, t) . Let \mathcal{G}_i denote the set of index pairs with the associated set of channel realizations $\mathcal{H}_{\mathcal{G}_i} = \{H_{f,t}, (f, t) \in \mathcal{G}_i\}$. Assuming a linear receiver, the crucial step in PHY abstraction in the literature [11]–[13] is to obtain an effective SINR $\bar{\rho}_i$ as follows.

$$\bar{\rho}_i = \alpha_1 I^{-1} \left(\frac{1}{n_{RE}} \sum_{(f,t) \in \mathcal{G}_i} I \left(\frac{\rho_{f,t,i}}{\alpha_2} \right) \right) \quad (9)$$

where $I()$ is a model-specific function, $\rho_{f,t,i}$ is the post-equalization SINR for UE i in the RE indexed by (f, t) , and α_1, α_2 are parameters that allow the model to adapt to the characteristics of the considered MCS. CESM corresponds to $I(x) = \log_2(1+x)$, EESM to $I(x) = e^{-x}$, LESM to $I(x) = \log_{10}(x)$, and MIESM to $I(x) = \mathcal{I}_m(x)$ where $\mathcal{I}_m(x)$ refers to the mutual-information (MI) between the input and the output in an AWGN channel with 2^m -QAM and an SNR of x . Following the computation of this effective SINR, a SINR-CER mapping is performed to obtain the error metrics. Currently, there is no clear consensus on which model-specific function to use, and more importantly, on how to use the above technique for non-linear receivers.

BMDR serves as a more natural metric for performing PHY abstraction. This is because the BMDR-CER relationship is clearer than the ESM-CER relationship, where the effective SINR is calculated using (9). We note that while BMDR is equivalent to MIESM for linear receivers, it can be applied to non-linear receivers as well. Our proposed approach is to calculate

$$\hat{R}_{\mathcal{D},i}(\mathfrak{m}, \mathcal{H}_{\mathcal{G}_i}) = \frac{1}{n_{RE}} \sum_{(f,t) \in \mathcal{G}_i} \hat{R}_{\mathcal{D},i}(\mathfrak{m}, H_{f,t}) \quad (10)$$

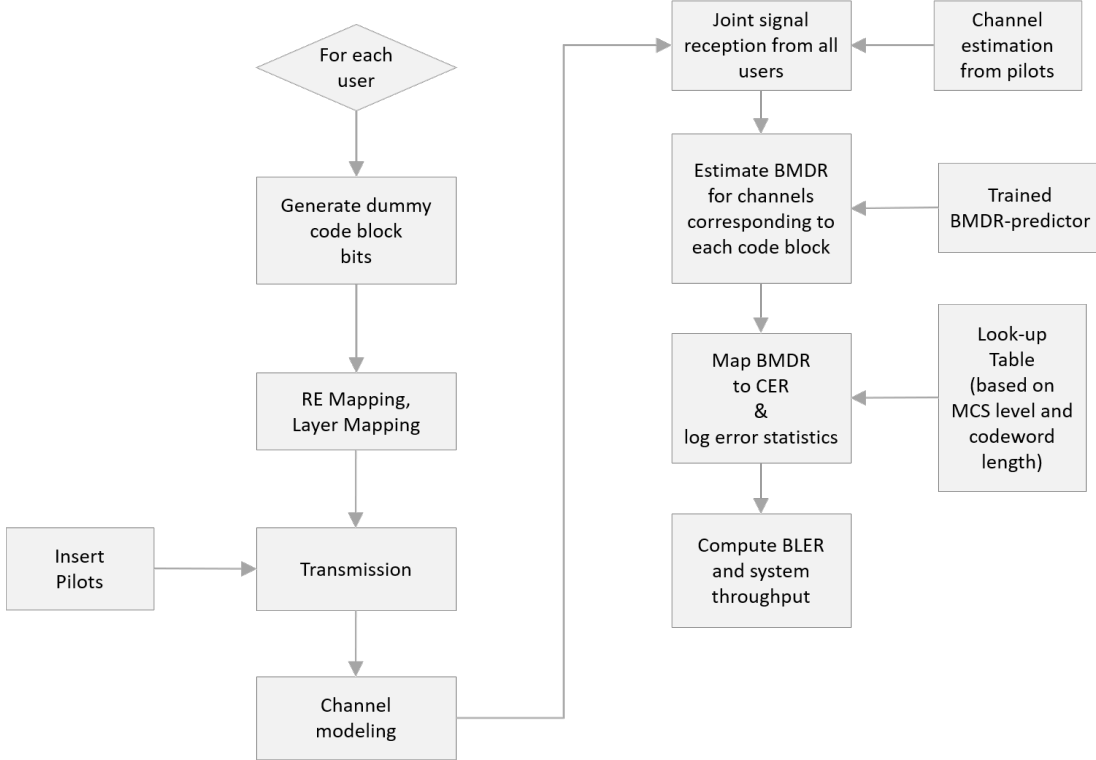


Fig. 3: Flowchart of the proposed PHY abstraction with the time-intensive procedures of Fig. 1 replaced by less complex procedures.

where $\mathbf{m} = \{m_1, \dots, m_{N_u}\}$ is the set of modulation orders used by all the co-scheduled users, and then map $\hat{R}_{\mathcal{D},i}(\mathbf{m}, \mathcal{H}_{\mathcal{G}_i})$ to a CER using the lookup table \mathcal{L}_U whose construction was detailed in Section III. With respect to 5G NR terminology [10], suppose that UE i notionally transmits B transport-blocks (TBs), with each TB being segmented into L CBs (a CB is a block of message bits). Therefore, a total of BL codewords are transmitted notionally (not actually transmitted because of the abstraction model). Then, the BMDR associated with each codeword transmission is estimated and mapped to a CER value from the lookup table. Let the estimated BMDR associated with the l^{th} codeword of TB j be $\hat{R}_{\mathcal{D},i}^{(j,l)}(\mathbf{m}, \mathcal{H}_{\mathcal{G}_i}^{(j,l)})$ where $\mathcal{H}_{\mathcal{G}_i}^{(j,l)}$ is the associated set of channel realizations, and let $\hat{p}_{i,j,l}$ denote the estimated CER for this codeword. Then,

$$\hat{p}_{i,j,l} = \arg \min_{P_e(R_{MLD}) \in \mathcal{L}_U} \left\{ \left| R_{MLD} - \hat{R}_{\mathcal{D},i}^{(j,l)}(\mathbf{m}, \mathcal{H}_{\mathcal{G}_i}^{(j,l)}) \right| \right\} \quad (11)$$

and the estimated probability of error for TB j is

$$\hat{P}_{i,j} = 1 - \prod_{l=1}^L (1 - \hat{p}_{i,j,l}). \quad (12)$$

MCS	(m, k, n)	SE	MCS	(m, k, n)	SE	MCS	(m, k, n)	SE
0	(2, 338, 2880)	0.23	10	(4, 1064, 2880)	1.48	16	(6, 1310, 2880)	2.73
1	(2, 444, 2880)	0.31	11	(4, 1220, 2880)	1.69	17	(6, 1452, 2880)	3.03
2	(2, 546, 2880)	0.38	12	(4, 1378, 2880)	1.91	18	(6, 1598, 2880)	3.33
3	(2, 708, 2880)	0.49	13	(4, 1552, 2880)	2.15	19	(6, 1732, 2880)	3.61
4	(2, 866, 2880)	0.60	14	(4, 1732, 2880)	2.41	20	(6, 1874, 2880)	3.90
5	(2, 1068, 2880)	0.74	15	(4, 1850, 2880)	2.57	21	(6, 2026, 2880)	4.22
6	(2, 1260, 2880)	0.88				22	(6, 2172, 2880)	4.53
7	(2, 1480, 2880)	1.03				23	(6, 2312, 2880)	4.82
8	(2, 1694, 2880)	1.18				24	(6, 2452, 2880)	5.11
9	(2, 1912, 2880)	1.33						

Fig. 4: The MCS table used for simulations.

The overall BLER for UE i is $\frac{1}{B} \sum_{j=1}^B \hat{P}_{i,j}$. The average system throughput can be estimated from the BLERs of all the users. Figure 3 shows the flowchart of the proposed technique.

VI. SIMULATION RESULTS

A. Simulation Setup

We consider the following setup for performing multi-cell, multi-link-level simulations, the code for which was written in NumPy [18] (for channel generation) and TensorFlow [19]. We consider 7 sites with 3 cells per site, leading to a total of 21 cells arranged in a hexagonal grid with wraparound (which essentially means that each cell sees an inter-cell interference pattern similar to that of the central cell). The inter-site distance is 200 m, and we consider the 38.901 Urban Micro (UMi) NLoS [20, Section 7.2] channel model. A total of 210 users are dropped at random in this grid. The carrier frequency is 3.5 GHz and each BS is equipped with a rectangular planar array consisting of 16 (2 vertical, 8 horizontal) single-polarized antennas installed at a height of 25 m and an antenna spacing of 0.5λ , where λ is the carrier wavelength. The UEs are each equipped with 2 dual-polarized antennas (1 vertical, 2 horizontal), and the maximum total output power P_{max} per UE is 23 dBm. We consider a regular 5G OFDM grid with a subcarrier spacing of 30 kHz, a slot of 14 symbols (of duration 35.7 μ s each), and 24 PRBs (of 12 subcarriers each) leading to a total usable system bandwidth of 8.64 MHz. Out of the 14 symbols, four are used for DMRS transmission and the remaining for data. The total uplink transmit power ρ (in

dBm) used by each UE is given by the following open-loop-power-control (OLPC) equation [21, Section 7]:

$$\rho = \min\{P_{max}, P_0 + 10 \log_{10} (N_{PRB}) + \alpha PL\} \quad (13)$$

where $P_{max} = 23$, $N_{PRB} = 24$ is the total number of PRBs, PL is the pathloss estimate (based on the measured channel gains on the downlink), P_0 is the expected received power per PRB under full pathloss compensation, and $\alpha \in [0, 1]$ is the fractional pathloss compensation factor. In our simulations, we take P_0 to be -98 dBm and $\alpha \in \{0.7, 1\}$. The transmission of each codeword is completed within each slot, so we fix the codeword length to be 2880 for all MCS levels. A custom MCS table as shown in Fig. 4 is used, where m refers to the modulation order, k to the message length, n to the codeword length, and $SE = mk/n$. 5G LDPC codes are used for channel coding.

Once the users are dropped, they are assumed to have a speed of 5 kmph, and the simulations are evaluated for 500 slots (of 0.5 ms each). The metrics are evaluated for ten such independent user drops. The number of transmitting layers is fixed to be four; so, depending on the users' positions, a single user can transmit using all of its four antennas, or four users can transmit using a single antenna each (and any combination of user antennas summing to four). The users are scheduled as follows: for each user, its serving cell is identified to be the one for which the average channel gains are the highest. Next, the $n_r \times n_r$ sized channel covariance matrix for each user is estimated at the BS using the SRS signals sent by the user, and is calculated by averaging over both time and frequency. Then, the set of users in each cell is divided into (not disjoint) subsets such that in each subset, the cross-correlation between the principal eigenvectors of the channel covariance matrices of any two users is less than 0.1. The cardinality of each subset is limited to four, and the subsets are served in a round-robin fashion. LMMSE channel estimation is performed for each user, and the interference covariance matrix at each cell is assumed to be perfectly known (i.e., with the notation as used in Section II, \mathbf{K}_n is assumed to be perfectly known while \mathbf{K}_e is estimated).

The BMDR-CER map is generated as explained in Section III using 100,000 codewords for each SNR, and the BMDR is computed using 10,000 independent input symbol and noise realizations for the same SNR in order to do the Monte-Carlo approximation of (4) for the SISO-AWGN channel.

For LLR generation, we consider the LMMSE detector as our choice of linear detector, and

the 32-best detector ($K = 32$ in [9], as explained in [1]) as our choice of non-linear detector. Their respective BMDR-predictors are trained as explained in [1, Section V]. We would like to reiterate that the reason for choosing the 32-best detector is due to its relatively low complexity compared to other non-linear techniques. In practice, it is often required to go beyond $K = 64$ in order to achieve significant performance gains over LMMSE. The purpose of our simulations is not to show that one detector is superior to the other, but rather to corroborate our claims about the role of BMDR in LA and PHY abstraction for both linear and non-linear detectors.

The throughput for each user in a given user drop, when using a particular detector, is obtained as follows: Suppose that UE i transmits a total of L_i codewords in that drop, with the j^{th} codeword carrying k_{ij} message bits. Let the total number of slots for that drop be T , with each slot being of duration t_{slot} seconds. Let $\delta_{ij} = 1$ if the j^{th} codeword is correctly decoded using the LDPC decoder for which the input LLRs are generated by the detector in context, and 0 otherwise. *We do not consider any type of automatic repeat request (ARQ) in our simulations.* Then, the throughput TP_i in megabits per second (Mbps) for UE i in that user drop is

$$TP_i = \frac{1}{10^6} \left(\frac{\sum_{j=1}^{L_i} \delta_{ij} k_{ij}}{T t_{slot}} \right). \quad (14)$$

The arithmetic mean (AM) and the geometric mean (GM) of the throughputs for all the users in a drop are then recorded, and this process is repeated for each of the ten independent drops. While the throughput for each user is heavily dependent on the user-scheduling algorithm, the goal here is to assess the performance of the detectors considered.

B. LA: Numerical Results

For MCS selection, we use the previous slot's channel realizations even if the users didn't transmit, except for the first slot in which case we estimate the first slot's channels before selecting the MCS. In addition to the two detectors, we also employ a hybrid one which selects either the LMMSE detector or the 32-best detector in each slot according to (8). We choose a target CER of 10^{-3} for MCS selection.

Figure 5 shows the plots of the average AM and GM throughputs for the three detectors along with the 90% confidence intervals (for different user drops). Figure 6 shows the percentiles of the CER for LMMSE and 32-best detector, so that for each CER value p_e on the X-axis, the corresponding value on the Y-axis indicates the percentage of users (across all drops) that achieved a CER less than or equal to p_e . For the case of $\alpha = 1$ (full path-loss compensation),

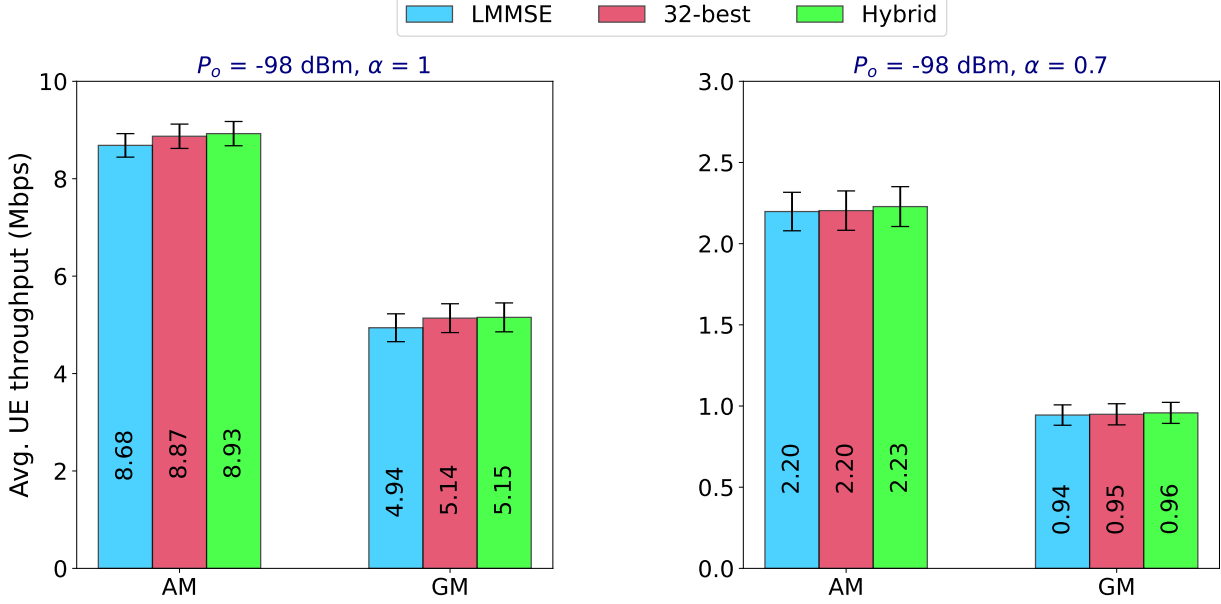


Fig. 5: The AM and GM throughputs with 90% confidence intervals for the three detection schemes for (left) $\alpha = 1$ and (right) $\alpha = 0.7$.

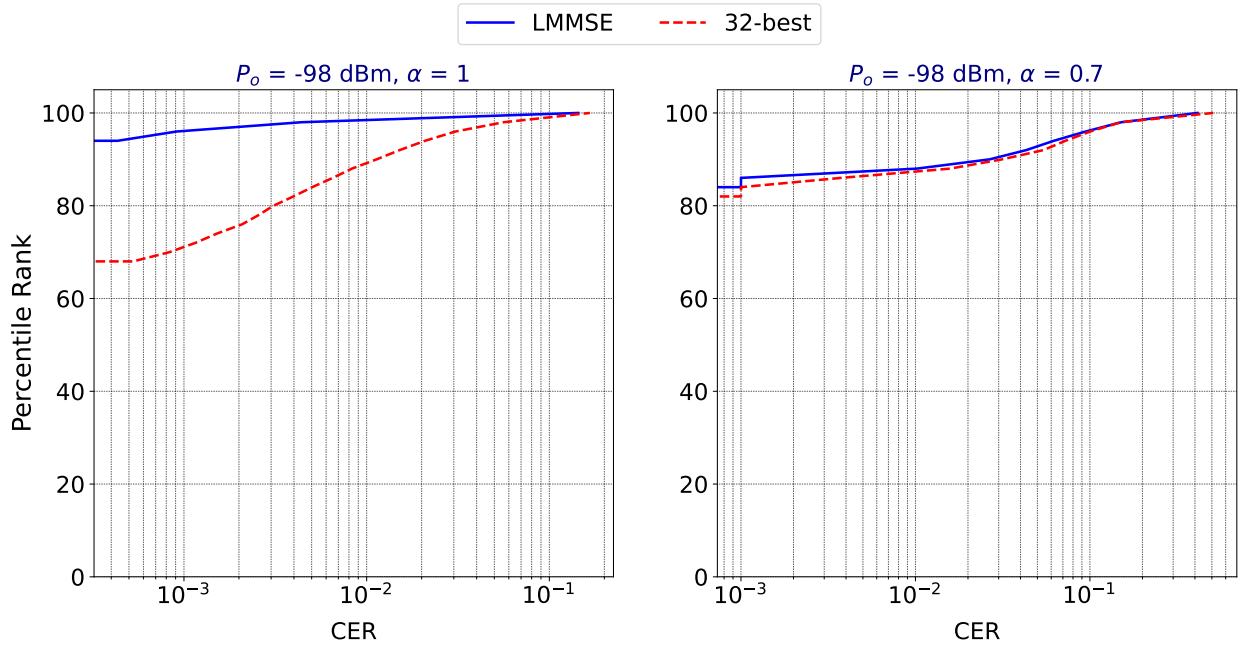


Fig. 6: The percentiles of the CER for the LMMSE detector and the 32-best detector for (left) $\alpha = 1$ and (right) $\alpha = 0.7$. For any CER value p_e on the X-axis, the corresponding value on the Y-axis indicates the percentage of users (across all drops) that achieved a $CER \leq p_e$.

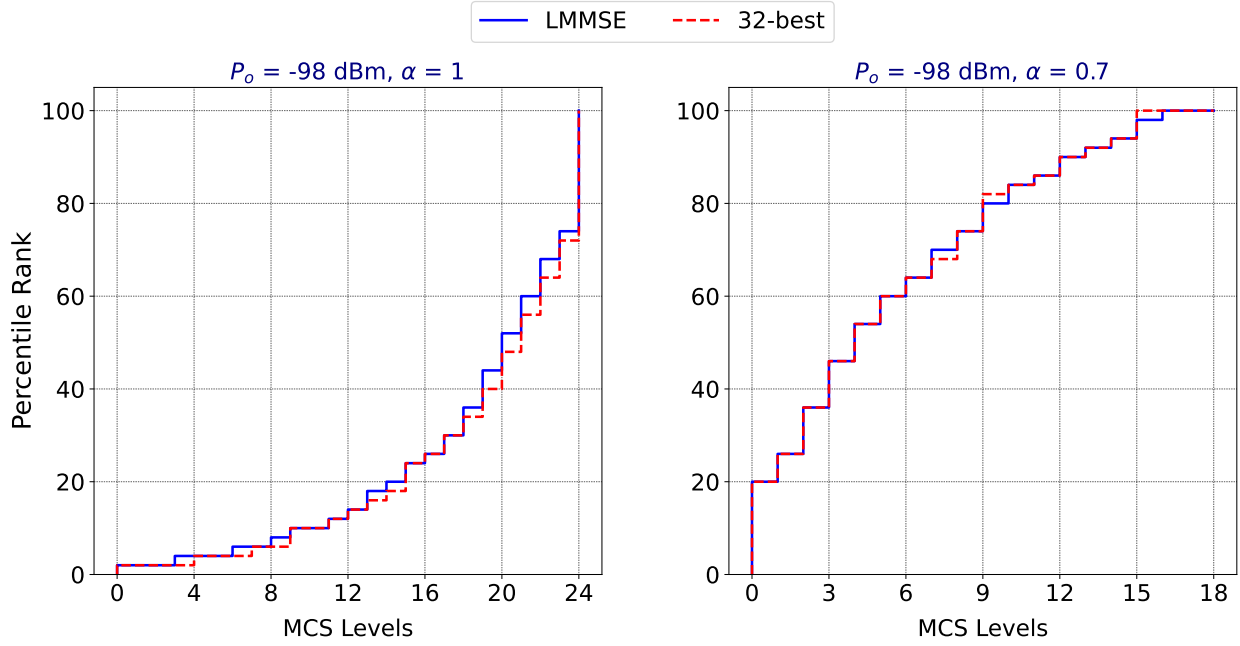


Fig. 7: The percentiles of the MCS levels for the LMMSE detector and the 32-best detector for (left) $\alpha = 1$ and (right) $\alpha = 0.7$.

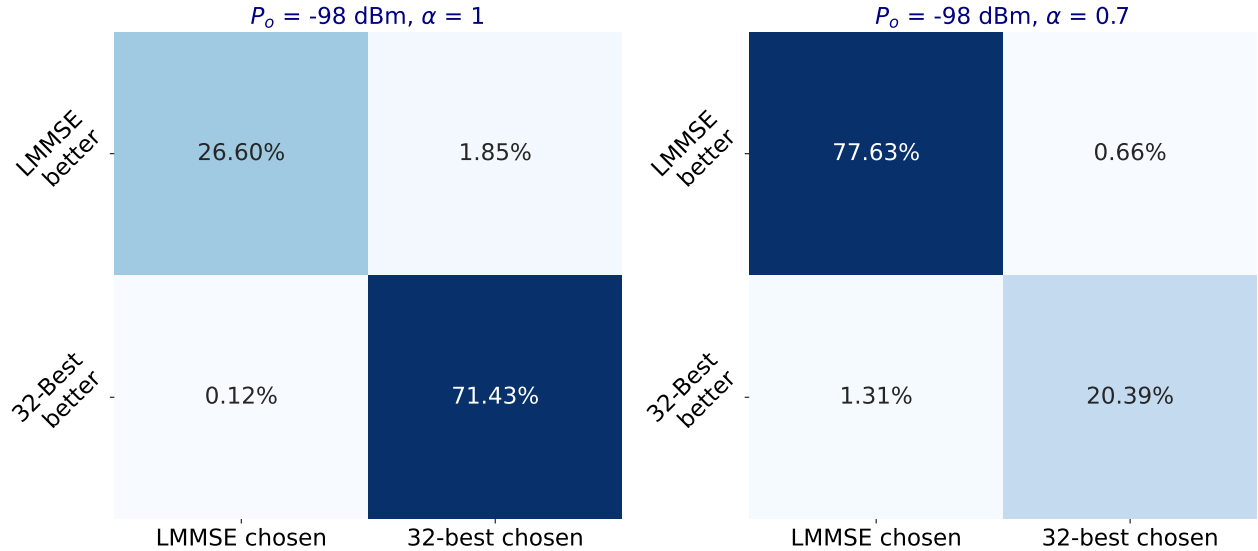


Fig. 8: The confusion matrix for detector selection using the proposed technique for (left) $\alpha = 1$ and (right) $\alpha = 0.7$.

users achieve the target CER with LMMSE detector around 94% of the time while this number is 68% for the 32-best detector. The reason for this difference, as highlighted in [1], is the ability to perform more accurate BMDR-prediction for a linear detector than for a non-linear detector, and is down to the accuracy of the trained BMDR-predictors. For the case of $\alpha = 0.7$ (partial path-loss compensation), the percentage of the time the CER target is met is around 82% for both the detectors. This is due to an increase in the usage of the lowest available MCS because the path-loss is not fully compensated. It might be that some users might not have sufficient SINR for error-free transmission even at the lowest MCS level. Figure 7, which shows the percentiles of the MCS levels used, highlights this.

It can be seen from Fig. 5 that the hybrid detector gives the best performance. Figure 8 shows the confusion matrices of the detector selection algorithm which corroborates the efficacy of the method. Since the 32-best detector uses only 32 survivors per layer in the search tree, there are scenarios where the LLRs might be overestimated due to the lack of a sufficient number of candidates of the opposite polarity for each transmitted bit. This leads to poorer performance compared to LMMSE in such cases. *Therefore, depending on the channel conditions, the hybrid detection scheme allows us to use a combination of a low-complexity detector and higher complexity non-linear detector for an overall better performance.*

C. PHY Abstraction: Numerical Results

We consider the same simulation setup as in the previous subsection, but do not perform data transmission, LLR-generation, or channel decoding. We follow the method outlined in the flowchart of Fig. 3 and compute the AM and GM throughputs using the BMDR-CER mapping. To be precise, the MCS levels are selected as in the previous subsection, and the estimated SE is multiplied by the mapped CER for each notional codeword transmission. This is then averaged for all users in all the drops. The computed AM and GM throughputs are plotted in Fig. 9, and the percentiles of the normalized UE-throughput estimation error are shown in Fig. 10. The latter is calculated as follows: if the actual UE throughput is TP_{actual} and the estimated throughput is TP_{est} , the normalized throughput estimation error is $|TP_{actual} - TP_{est}|/TP_{actual}$. Also marked in Fig. 10 are the 95th and 99th percentiles of the normalized estimation errors for both LMMSE and 32-best detector. The high deviations are for UEs with very low throughput (possibly cell-edge UEs for $\alpha = 0.7$, or due to low MCS levels in the case of $\alpha = 1$). In Fig. 11, we present the CER plots as a function of UE transmit power in a link-level simulation setting. We consider

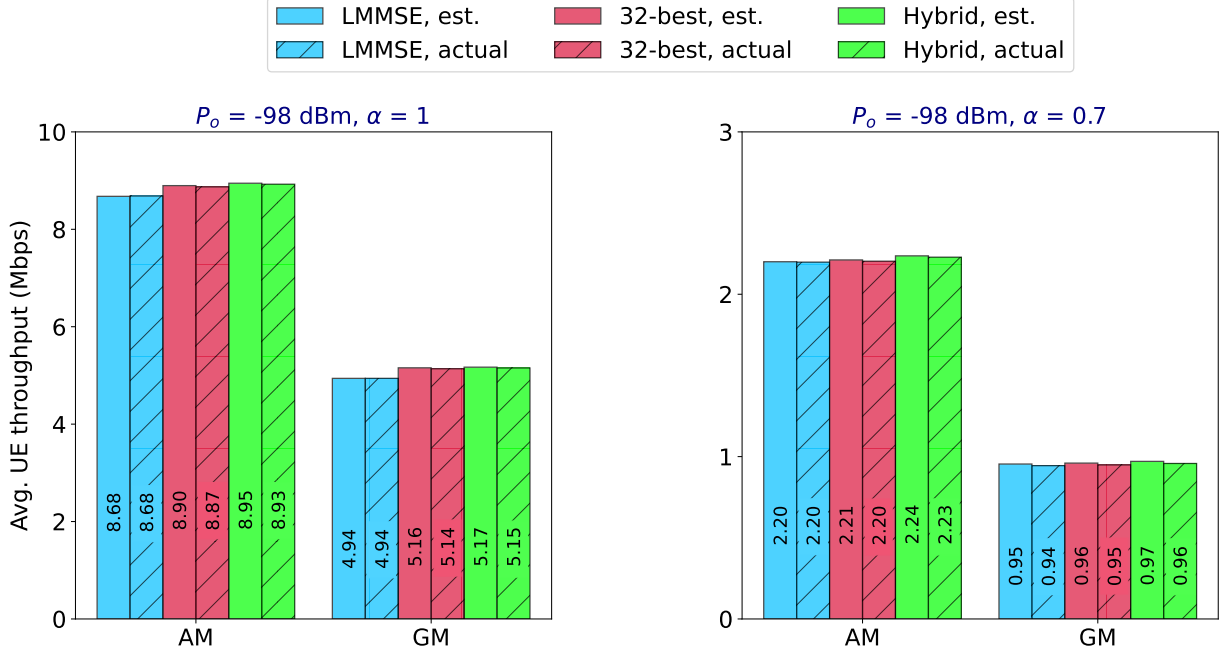


Fig. 9: The AM and GM for the three detector schemes using PHY abstraction (compared with the actual values corresponding to Fig. 5) for (left) $\alpha = 1$ and (right) $\alpha = 0.7$.

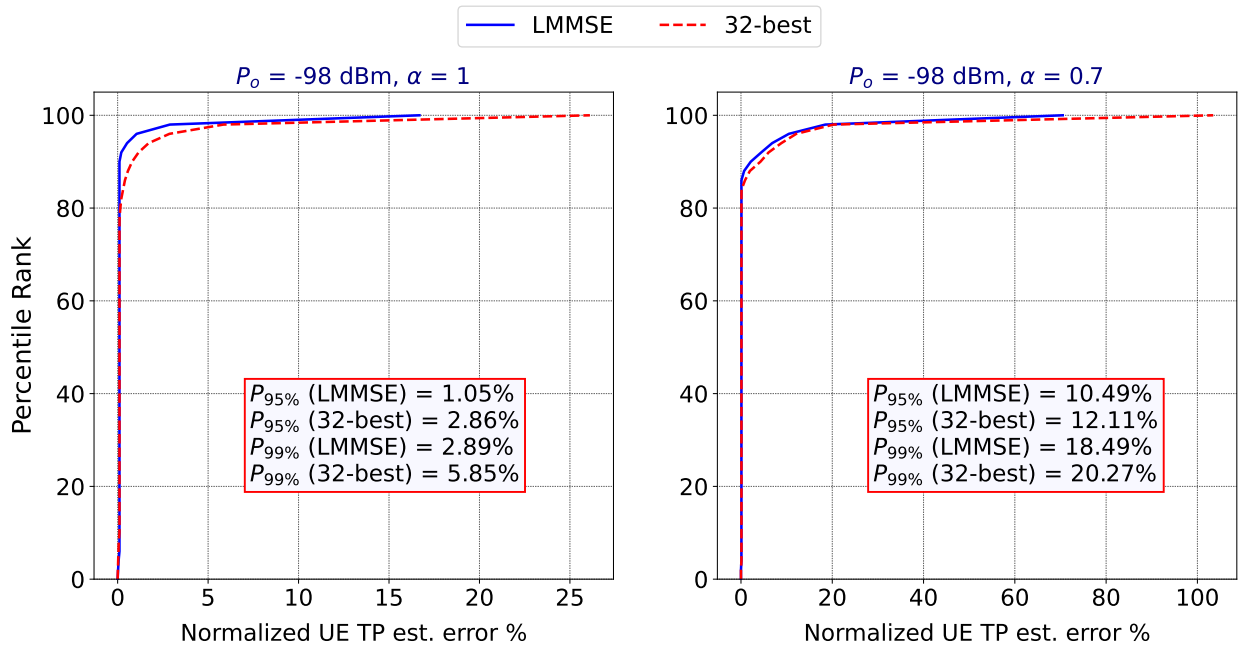


Fig. 10: The percentiles of the normalized UE-throughput estimation error using PHY abstraction for the LMMSE detector and the 32-best detector for (left) $\alpha = 1$ and (right) $\alpha = 0.7$.

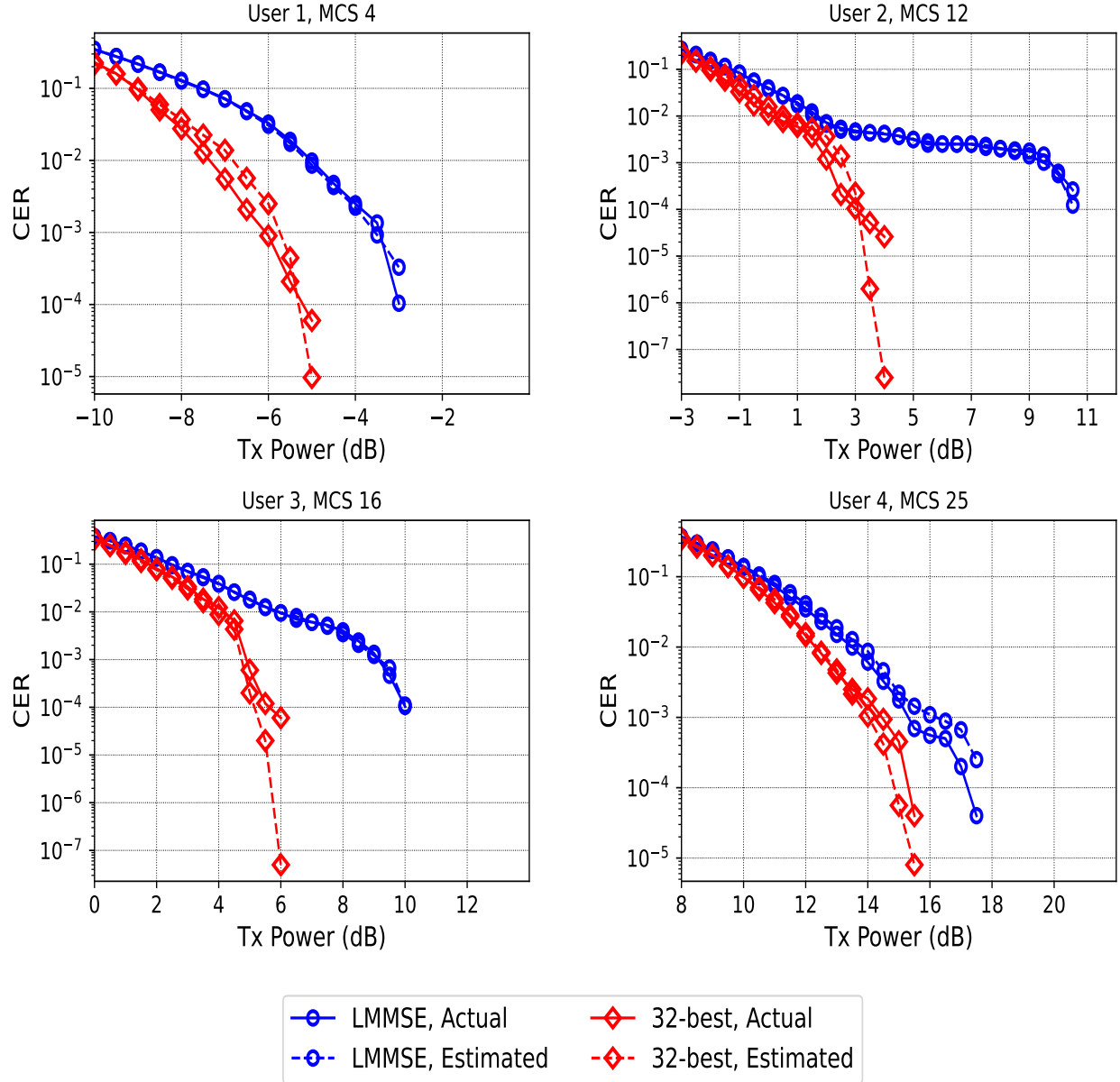


Fig. 11: The link-level CER v. transmit power (dB) plots for the LMMSE detector and the 32-best detector for four UEs with different MCS levels. The solid lines correspond to the actual CERs and the dashed lines to the CERs estimated using the proposed abstraction technique.

four users with different MCS levels. The number of transmitted codewords is limited to 10,000 and hence, the estimated CERs deviate a little at values below 10^{-5} . However, the plots show that the proposed link-level modeling is quite useful in capturing the main behavior of the PHY components.

VII. DISCUSSION AND CONCLUDING REMARKS

In the second part of this two-part paper, we proposed a new algorithm for uplink link-adaptation in MU-MIMO systems that use arbitrary receivers. This algorithm was shown to rely on the concepts of BMDR developed in the first part, and its efficacy was shown for the case of both a linear and a non-linear detector. We also proposed a hybrid strategy that dynamically selects the most suitable detector from a list of available detectors for improved performance. We next proposed a technique to perform PHY abstraction in MU-MIMO systems for arbitrary receivers. The proposed technique allows a simpler evaluation of complex (possibly non-linear) receiver algorithms without compromising significantly on the accuracy of the performance metrics.

The most computation-intensive task in both the applications is the offline training of the BMDR-predictor for non-linear detectors. However, this is a one-time process. Non-linear detectors are playing an increasingly important role in advanced wireless technologies, especially with the advent of machine-learning based receivers. As the uplink traffic is expected to increase significantly in the future, we expect the concepts developed in this paper to be very useful in the next-generation wireless technologies. Further, one might even consider the usage of BMDR in other applications such as user-pairing and scheduling.

ACKNOWLEDGEMENT

The authors would like to thank Harish Vishwanath, Suresh Kalyanasundaram, K. S. Karthik, and Chandrashekhar Thejaswi for valuable discussions on the topic, and Sivarama Venkatesan for providing a NumPy-based 3GPP channel-modeling package.

REFERENCES

- [1] K. P. Srinath and J. Hoydis, “Bit-Metric Decoding Rate in Multi-User MIMO Systems: Theory,” 2022. [Online]. Available: <https://arxiv.org/abs/2203.06271>
- [2] P. Bertrand, J. Jiang, and A. Ekpenyong, “Link Adaptation Control in LTE Uplink,” in *2012 IEEE Vehicular Technology Conference (VTC Fall)*, 2012, pp. 1–5.

- [3] M. G. Sarret, D. Catania, F. Frederiksen, A. F. Cattoni, G. Berardinelli, and P. Mogensen, "Dynamic Outer Loop Link Adaptation for the 5G Centimeter-Wave Concept," in *Proceedings of European Wireless 2015; 21st European Wireless Conference*, 2015, pp. 1–6.
- [4] S. Sun, S. Moon, and J.-K. Fwu, "Practical Link Adaptation Algorithm With Power Density Offsets for 5G Uplink Channels," *IEEE Wireless Communications Letters*, vol. 9, no. 6, pp. 851–855, 2020.
- [5] D. Tse and P. Viswanath, *Fundamentals of Wireless Communication*. USA: Cambridge University Press, 2005.
- [6] E. Viterbo and J. Boutros, "A Universal Lattice Code Decoder for Fading Channels," *IEEE Trans. Inf. Theory*, vol. 45, no. 5, pp. 1639–1642, 1999.
- [7] C. Studer and H. Bölskei, "Soft–Input Soft–Output Single Tree-Search Sphere Decoding," *IEEE Trans. Inf. Theory*, vol. 56, no. 10, pp. 4827–4842, 2010.
- [8] L. G. Barbero and J. S. Thompson, "Fixing the Complexity of the Sphere Decoder for MIMO Detection," *IEEE Trans. Wireless Commun.*, vol. 7, no. 6, pp. 2131–2142, 2008.
- [9] Z. Guo and P. Nilsson, "Algorithm and Implementation of the K-best Sphere decoding for MIMO Detection," *IEEE J. Sel. Areas Commun.*, vol. 24, no. 3, pp. 491–503, 2006.
- [10] 3GPP, "NR; Multiplexing and channel coding," 3rd Generation Partnership Project (3GPP), Technical Specification (TS) 38.212, 12 2020, version 16.4.0. [Online]. Available: <https://portal.3gpp.org/desktopmodules/Specifications/SpecificationDetails.aspx?specificationId=3214>
- [11] K. Brueninghaus, D. Astely, T. Salzer, S. Visuri, A. Alexiou, S. Karger, and G.-A. Seraji, "Link performance models for system level simulations of broadband radio access systems," in *2005 IEEE 16th International Symposium on Personal, Indoor and Mobile Radio Communications*, vol. 4, 2005, pp. 2306–2311 Vol. 4.
- [12] L. Wan, S. Tsai, and M. Almgren, "A fading-insensitive performance metric for a unified link quality model," in *IEEE Wireless Communications and Networking Conference, 2006. WCNC 2006.*, vol. 4, 2006, pp. 2110–2114.
- [13] S. Lagen, K. Wanuga, H. Elkotby, S. Goyal, N. Patriciello, and L. Giupponi, "New radio physical layer abstraction for system-level simulations of 5g networks," in *ICC 2020 - 2020 IEEE International Conference on Communications (ICC)*, 2020, pp. 1–7.
- [14] G. Caire, G. Taricco, and E. Biglieri, "Bit-Interleaved Coded Modulation," *IEEE Trans. Inf. Theory*, vol. 44, no. 3, pp. 927–946, May 1998.
- [15] M. Cirkic, D. Persson, and E. G. Larson, "Allocation of Computational Resources for Soft MIMO Detection," *IEEE J. Sel. Topics in Signal Process.*, vol. 5, no. 8, pp. 1451–1461, 2011.
- [16] S. Chaudhari, H. Kwon, and K. Song, "Reliable and Low-Complexity MIMO Detector Selection using Neural Network," in *Int. Conf. Comput., Netw. and Commun. (ICNC) 2020*, 2020, pp. 608–613.
- [17] H. Kwon and K. Song, "MIMO-OFDM Detector Selection using Reinforcement Learning," in *Int. Conf. Comput., Netw. and Commun. (ICNC) 2020*, 2020, pp. 347–352.
- [18] C. R. Harris, K. J. Millman, S. J. van der Walt, R. Gommers, P. Virtanen, D. Cournapeau, E. Wieser, J. Taylor, S. Berg, N. J. Smith, R. Kern, M. Picus, S. Hoyer, M. H. van Kerkwijk, M. Brett, A. Haldane, J. F. del Río, M. Wiebe, P. Peterson, P. Gérard-Marchant, K. Sheppard, T. Reddy, W. Weckesser, H. Abbasi, C. Gohlke, and T. E. Oliphant, "Array programming with NumPy," *Nature*, vol. 585, no. 7825, pp. 357–362, Sept. 2020. [Online]. Available: <https://doi.org/10.1038/s41586-020-2649-2>
- [19] M. Abadi, A. Agarwal, P. Barham, E. Brevdo, Z. Chen, C. Citro, G. S. Corrado, A. Davis, J. Dean, M. Devin, S. Ghemawat, I. Goodfellow, A. Harp, G. Irving, M. Isard, Y. Jia, R. Jozefowicz, L. Kaiser, M. Kudlur, J. Levenberg, D. Mané, R. Monga, S. Moore, D. Murray, C. Olah, M. Schuster, J. Shlens, B. Steiner, I. Sutskever, K. Talwar, P. Tucker, V. Vanhoucke, V. Vasudevan, F. Viégas, O. Vinyals, P. Warden, M. Wattenberg, M. Wicke, Y. Yu, and X. Zheng,

“TensorFlow: Large-Scale Machine Learning on Heterogeneous Systems,” 2015, software available from tensorflow.org. [Online]. Available: <https://www.tensorflow.org/>

[20] 3GPP, “Study on channel model for frequencies from 0.5 to 100 GHz,” 3rd Generation Partnership Project (3GPP), Technical Specification (TS) 38.901, 12 2019, version 16.1.0. [Online]. Available: <https://portal.3gpp.org/desktopmodules/Specifications/SpecificationDetails.aspx?specificationId=3173>

[21] ——, “NR; Physical layer procedures for control,” 3rd Generation Partnership Project (3GPP), Technical Specification (TS) 38.213, 12 2021, version 17.0.0. [Online]. Available: <https://portal.3gpp.org/desktopmodules/Specifications/SpecificationDetails.aspx?specificationId=3215>